Impact of branch reorientation on breaking stress in *Liriodendron tulipifera* L.

Jason W. Miesbauer [a,*], Edward F. Gilman [b], Forrest J. Masters [c], Sangam Nitesh [d]

[a] The Morton Arboretum, 4100 Illinois Route 53, Lisle, IL 60532, USA
[b] Environmental Horticulture Department, 1543 Fifield Hall, University of Florida, Gainesville, FL 32611, USA
[c] Engineering School for Sustainable Infrastructure and Environment, 365 Weil Hall, University of Florida, Gainesville, FL 32611, USA
[d] Civil and Costal Engineering Department, 365 Weil Hall, University of Florida, Gainesville, FL 32611, USA

ARTICLE INFO

ABSTRACT

It has been observed that during ice, snow, and wind storms, branches oriented vertically tend to incur more damage than branches oriented horizontally. A study was conducted to determine breaking stress and breaking position of branches reoriented nearly horizontal and nearly vertical. Branches oriented 40–50° from horizontal with mean diameter 4.9 cm (SD ± 0.73) were removed from two trees and transferred to a custom branch pulling station. Branches were reoriented either nearly horizontal (76–89°) or vertical (6–29°) to a reinforced vertical post. Branches were pulled vertically downward from three equidistant positions along the branch until they broke. Failure stress for horizontal oriented branches (64 MPa) was double the stress required to pull vertical oriented branches to failure (32 MPa). Nine of ten horizontal branches failed between the branch base and the pull point closest to the base (proximal pull point); whereas seven of ten vertical branches failed farther from the base, between the proximal and middle pull points. Average length from branch base to failure point for horizontal branches was 12.8 cm, and 74.6 cm for vertical branches. Despite requiring less stress to break, branch angle change at the distal and middle pull points from the original position to the position at failure for vertical branches was greater than for horizontal branches; whereas angle change at the proximal pull point was greater for horizontal branches. Branch taper was not different between reorientation treatments. Implications on pruning strategies are discussed.

© 2014 Elsevier GmbH. All rights reserved.

Introduction

Every year trees are damaged during storms, causing billions of dollars in property damage in the United States as well as 407 human fatalities from 1995 to 2007 (Schmidlin, 2009). Observations on certain species during ice, snow, and wind storms, suggest that upright oriented branches may incur more damage than horizontally oriented branches (Hauer et al., 1993), however there are few studies supporting this observation. Many factors including branch attachment angle from the trunk (Rebertus et al., 1997), proximity to other branches and trees (Duryea et al., 2007), crown position (Bruederle and Stearns, 1985), age (Hauer et al., 1993), and anatomical or physiological branch attributes (Dahle and Grabosky, 2010) may contribute to branch breakage.

Some of the variation in breakage might be attributed to differences in branch wood properties, such as occurrence of reaction wood. In angiosperms, reaction wood is referred to as tension wood, and develops primarily on the upper side of branches and leaning stems. Branches that are oriented more horizontally are subject to larger gravitational force than upright growing branches, and gravitational stimulus is a primary trigger for reaction wood formation (Wilson and Archer, 1977; Du and Yamamoto, 2007). Yet the direct impact of branch attachment angle on presence of reaction wood and strength attributes is not clear, and not all trees develop reaction wood. For example, only about half of 122 tree species surveyed by Fisher and Stevenson (1981) had branches that contained reaction wood. Furthermore, they reported that tension wood formation varied considerably among trees of a given species, and even within individual trees due to factors such as tree architecture and branch angle.

Common measures of material properties such as modulus of elasticity (*E*) and modulus of rupture (MOR) are used in wood science research (Haygreen and Bowyer, 1996; Green, 2001). *E* is a measure of stiffness as indicated by its resistance to bending

* Corresponding author. Tel.: +1 920 419 0183; fax: +1 630 719 2433.
E-mail addresses: jmiesbauer@mortonarb.org (J.W. Miesbauer), egilman@ufl.edu (E.F. Gilman), masters@ce.ufl.edu (F.J. Masters), sangam.desou@ufl.edu (S. Nitesh).

within the elastic range (Morgan and Cannell, 1988; Niklas, 1992); whereas MOR is the bending stress required to cause failure in standardized bending tests, and has been used as a measure of strength (USDA Forest Service, 2010). Material properties can vary considerably between species, among individuals within a single species, and within individual trees (Niklas, 1997; Menuccini et al., 1997; Sone et al., 2006). Most standardized tests on wood material properties are performed on clear, defect-free samples extracted from trunks that are either dried or green (USDA Forest Service, 2010). Material properties of these samples, however, may not accurately reflect whole tree or branch response to bending (Putz et al., 1983; Ruel et al., 2010). Extrapolating data obtained from dried samples is problematic because moisture content affects wood material properties (Niklas, 1997). Most research on wood material properties has focused on trunk wood, while few have measured samples extracted from branches (Kane, 2007; Gurau et al., 2008; Dahle and Grabosky, 2010). Kane (2007) found that E and MOR of samples extracted from branches pulled to failure had no influence on branch breaking stress in *Pyrus calleryana* Decne. var. 'Bradford'. Tension wood E of samples extracted from trunk wood was reported to be generally, but not always, higher than normal wood E (Coutand et al., 2004; Ruelle et al., 2007). However, Dahle and Grabosky (2010) found no difference in E between branch wood samples with and without tension wood. Furthermore, tension wood has less compression strength than normal wood (USDA Forest Service, 2010; Ruelle et al., 2011). Given the apparent complexity of tree response, it is difficult to determine what effect, if any, tension wood and attachment angle have on branch failure.

Several studies employed pulling techniques on intact branches to evaluate branch union strength (Lilly and Sydnor, 1995; Gilman, 2003; Dahle et al., 2006). Unions with a small branch:trunk diameter (aspect) ratio were stronger than unions with an aspect ratio closer to one, and branch angle typically correlated poorly with attachment strength (Gilman, 2003; Kane, 2007; Kane et al., 2008). In contrast, MacDaniels (1923) reported wide branch unions to be stronger. Branches with wider angles of attachment appear to be less likely to develop bark inclusions (MacDaniels, 1923; Shigo, 1985), which reduce attachment strength (Smiley, 2003). Furthermore, trees with an excurrent form, with a dominant central leader and smaller, branches that are oriented approximately horizontal, may have an increased resistance to damage in wind storms (Sellier and Fourcaud, 2009) and trees with an excurrent form and wide branch angles experienced less damage in an ice storm (Hauer et al., 1993) and wind storms (Duryea et al., 2007). Despite the abundance of work relating branch orientation (attachment angle) to union strength, impact of branch orientation on breaking stress of the branch itself is poorly understood. Branches in previous studies were pulled from a single point, usually near the branch union, which may not simulate natural loading associated with snow or ice.

The primary objective of this study was to compare the mechanical stress required to break branches artificially reoriented approximately vertical with that of branches reoriented horizontally. We sought to isolate the impact of orientation on failure while minimizing potential differences in mechanical, anatomical, and physiological properties of sampled branches by selecting branches that were naturally displayed on sample trees in a very narrow attachment angle range (40–50°) and reorienting them during testing. A better understanding of how mechanical stress, induced by spatially distributed loads, causes failure in tree branches could help guide tree pruning strategies designed to reduce risk. The second objective was to evaluate a new three-point pulling methodology in an effort to more closely simulate the spatial load distribution naturally occurring in ice, snow and some strong wind events.


Fig. 1. Branch mounting bracket and branch secured to vertical post.

Materials and methods

Three-point pull system validation

A test was designed to determine if a three-point pull test could mimic the branch deflection that occurred under static loading as might be encountered during a natural vertical loading event. Branches were selected from two *Liriodendron tulipifera* L. trees located at the Environmental Horticulture Landscape Experimental Laboratory at the University of Florida in Gainesville (29.4° N, 82.2° W, USDA hardiness zone 8a). Trees were approximately 13 m tall with a DBH of 38 and 41 cm. To minimize mechanical, anatomical, and physiological variation among branches, only those with attachment angles (angle formed between the branch and the trunk above) between 40 and 50° were sampled. The top of each branch was marked to indicate its position relative to vertical. Four branches (2 per tree) with a diameter range 4.7–5.3 cm (mean = 5.0 cm, SD ± 0.25) and length range 4.11–4.47 m (mean = 4.28 m, SD ± 0.16) were removed from trees one at a time by cutting them perpendicular to the top of the branch just beyond the branch collar and taken to the on-site indoor lab. They were placed into a custom mounting bracket which secured the basal 15 cm of the branch (Fig. 1) with the top surface positioned on top as it was in the tree. A 2.5 cm-wide ratchet strap secured the branch to the plate of the bracket to prevent twisting and pull-out. Two pieces of 15 cm long by 7.5 cm wide angle iron secured the top and bottom of the branch base. The sections of angle iron were secured to the steel plate with two bolts each. The steel plate had vertical channels where the bolts secured the angle iron, allowing the angle iron adjust for differences in branch diameter. Two c-clamps tightly secured the angle iron to the top and bottom of the branch. A 15 cm long by 4 cm wide plate of steel was secured longitudinally along the branch base with a c-clamp to prevent the branch from being pulled laterally out of the bracket during testing. The mounting bracket was secured to a solid vertical structure and branches were reoriented either approximately horizontal (79.4 and 86.2°) or approximately vertical (12.1 and 14.6°). Angles were measured by placing a 16.5 cm-long digital level (SmartTool™, M-D Building Products, Oklahoma City, OK, USA), accurate to one-tenth of a degree, on the top of each branch distally adjacent to the mounting bracket. The single light source in the room pointed directly at the branch, casting a distinct shadow onto the wall 1 m away. The outline of the primary branch was traced onto paper secured to the wall. The primary branch was identified by following the larger of two branches where bifurcations or lateral branches occurred.

Three loading points were selected: (1) proximal – immediately proximal to the first major branch union (defined as having a
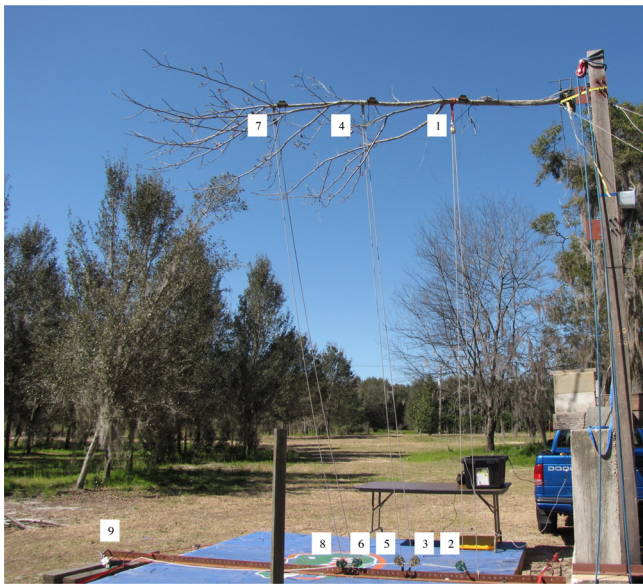
Fig. 2. Three-point pulley system at branch pulling station just prior to pulling horizontal branch.

diameter at least one-third the diameter of the primary branch), (2) distal – at the point where primary branch diameter was 2.5 cm, and (3) middle – the mid-point along the primary branch between them. The distal pull point diameter was set at 2.5 cm because tree care professionals typically regard storm damage to branch tips with a smaller diameter than this as insignificant. A 13 mm-wide webbing sling (27 kN breaking strength) (BlueWater, Carrollton, GA, USA) was girth hitched to the primary branch at each loading point and a Kong Slideline carabiner (24 kN capacity) (Kong, Monte Marenzo, Italy) was attached to each webbing sling. To simulate natural deflection patterns under static vertical load, a 0.91 kg mass was attached to each carabiner. After two minutes, branch deflection stopped changing and the outline of the primary branch shadow was traced on the paper with a fine black marker. A second set of 0.91 kg weights were added at the same three points and allowed to suspend for two minutes when all movement stopped. The branch shadow was traced again. The same process was repeated a third time, with the final mass totaling 2.73 kg applied at each of the three points. Weights were removed and the branch returned to its original position.

A custom three-point pull system was developed to mimic the branch deflection that resulted from application of the three static weights. A 5 m long, 15 cm × 15 cm square wood beam (136 kg) was placed on the indoor lab concrete floor parallel to and directly under the branch. A 5 m long, 5 cm × 5 cm strip of angle iron was secured to the entire length of the beam in a manner similar to that shown in Fig. 2 (bottom). The angle iron had 13 mm diameter holes pre-drilled every 5 cm along its entire length. A 32 mm sheave-diameter micro pulley (32 kN capacity) (CMI, Franklin, WV, USA) was attached to each of the 3 carabiners along the branch. A 7.9 mm diameter low-stretch rope (Lehigh, Macungie, PA) was tied to the hole in the angle iron directly below the proximal pull point. The free end of the rope was fed through the proximal pulley (pulley 1) on the branch and back down toward the angle iron. The rope was fed through a 61 mm sheave-diameter pulley (27 kN capacity) (CMI, Franklin, WV, USA) (pulley 2), which was attached to the angle iron with a 28 kN capacity Petzl AM'd Tri Act (Petzl, Crolles, France) carabiner in the hole immediately distal to the hole where the rope was tied. The rope was fed through pulley 3, which was attached with a carabiner to the angle iron directly under the middle pull point on the branch, up through pulley 4 at the

middle pull point on the branch, and back down toward the angle iron. The rope was then fed through pulley 5, which was attached to the angle iron with a carabiner in the hole distally adjacent to pulley 3. The rope was fed through pulley 6, which was attached to the angle iron with a carabiner directly under the distal pull point, up through the distal pulley (7) on the branch, and back down toward the angle iron. The rope was then fed through pulley 8, which was attached to the angle iron in the hole distally adjacent to pulley 6. The rope was fed through pulley 9, which was attached to the terminal end of the angle iron with a carabiner and turned 90° to the side, perpendicular to the angle iron and parallel to the floor. The mass of the rope and pulley system caused no perceptible branch deflection. Pulleys attached to the branches (1, 4, and 7) were all the same specifications as described for pulley 1. Pulleys attached to the angle iron (2, 3, 5, 6, 8, and 9) were all of the same specifications as described for pulley 2.

The free end of the rope was slowly pulled by hand, causing the branch to deflect from its original position. Pulling was stopped when the shadow of the branch appeared to match the branch outline from the first static weight application. The rope was tied off with the branch in this position and the outline of the shadow was traced with a fine red marker. Pulling of the rope then continued until the shadow of the branch appeared to match the outline of the second static weight application. The rope was again tied off with the branch in this position and the outline of the shadow was traced. Pulling resumed until the branch shadow appeared to match the outline of the third static weight application. The rope was tied off with the branch in this position and the shadow outline was again traced. Tension was released from the rope and the branch returned to its original position.

Branch deflection from the pre-loading start position was measured at 8 locations spaced at 30 cm intervals along the primary branch length of each traced outline, starting at the proximal pull point. The distance of horizontal deflection was measured for the vertical oriented branches, and the distance of vertical deflection was measured for the horizontal oriented branches. Three-way factorial analysis of variance (ANOVA) was performed to test differences in branch deflection for load method (static loading vs. three-point pull system), location (8 positions) along branch, and static mass (first, second, or third application of 0.91 kg). Separate analyses were performed for vertical and horizontal branches because deflection measurement directions were different for each orientation treatment. Analysis was performed using the PROC GLM procedure in SAS version 9.2 (SAS Institute, Cary, NC).

Load distribution test

A load distribution test conducted prior to the branch pull test measured the force applied at each of the three pull points while pulling branches to failure. This test was conducted so that load cells would not have to be attached to branches during the twenty branch pull tests. This minimized mass of instrumentation and eliminated risk of damage to instruments when branches potentially failed dramatically and fell to the ground.

An outdoor branch pulling station was constructed on-site (Fig. 2). To simulate a tree trunk, a 5 m tall, vertical 15 cm × 15 cm square wood post was secured to a pre-existing 1.7 m tall × 3 m long × 0.5 m thick concrete wall (visible in Fig. 2, bottom right). To prevent the post from bending while branches were pulled, two guy wires secured to the ground were attached to the top of the post. Horizontal lines were drawn on the post at 30 cm increments as a scale for measuring distance from ground to each pull point and break point by video recording. A 3.7 m × 3.7 m wooden platform was situated on the ground at the base of the concrete wall to create a flat surface. The aforementioned angle iron was secured to the platform in a north–south orientation, parallel to and below
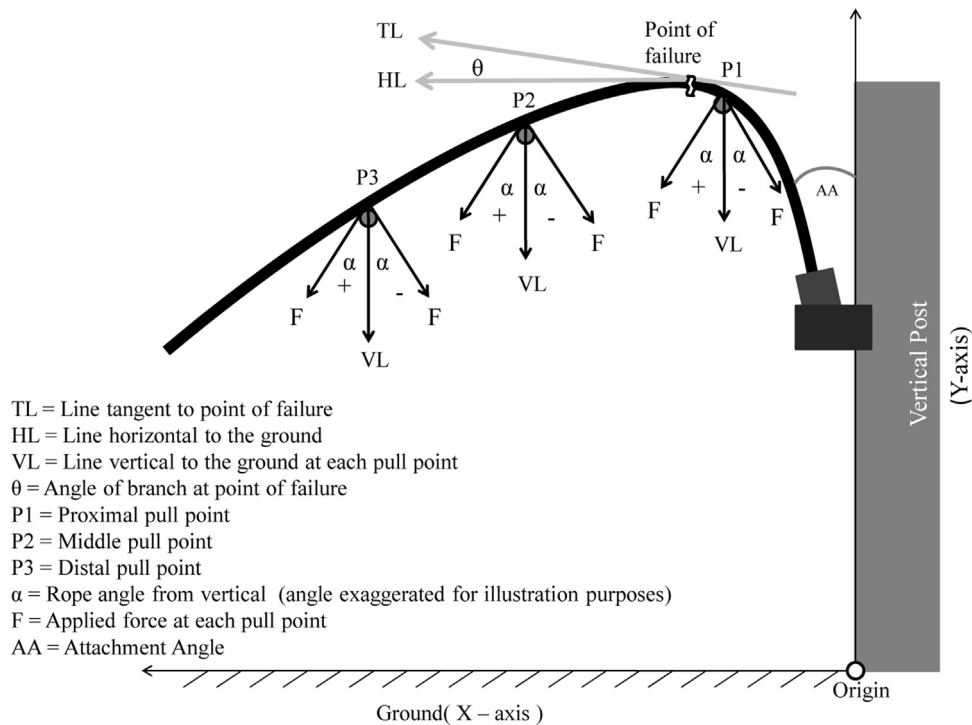
Fig. 3. Diagram of vertical branch at failure.

mounted branches. The platform was secured to the ground with ratchet straps attached to concrete ground anchors.

Four branches with a diameter range 5.2–6.1 cm (mean = 5.8 cm, SD ± 0.39) and length range 4.6–5.0 m (mean = 4.8 m, SD ± 0.17) were used for load cell calibration ($n = 2$ each of horizontal and vertical orientation). Branches were selected from the same trees based on the same parameters described for the three-point pull system validation test. Branches were removed from the trees, and immediately secured in the custom mounting bracket at the pulling station (Fig. 1). The bracket was then bolted to a steel mounting plate on the post so that branches pointed south, parallel to the angle iron below. Distance between the ground and the mounting plate was 3.5 m for vertically oriented branches and 5 m for horizontally oriented branches so pulled branches would not contact the ground. Primary branch diameter was measured at each of the three predetermined pull points prior to securing webbing slings and carabiners at each point as previously mentioned. A 226.8 kg capacity S-type load cell (Interface, Scottsdale, AZ, USA) was attached to each carabiner. A micro pulley was attached to the opposite end of each load cell with a Kong Slideline carabiner.

Pulleys were attached to the angle iron and the rope was fed through the pulley system as described previously, with two exceptions. First, pulleys were attached to the angle iron at a point where they would be approximately below the branch pull points when the branches were expected to fail (rather than attaching pulleys directly below the starting branch pull points). Therefore, pulleys for horizontal oriented branches were closer to the post than for vertical oriented branches. Secondly, the terminal pulley (Fig. 2, pulley 9) was attached to a 2268 kg capacity S-type load cell (Interface, Scottsdale, AZ, USA), which was secured to the terminal end of the angle iron with a 28 kN capacity Petzl AM'd Tri Act carabiner.

After the rope ran through the terminal pulley it turned 90° to the east parallel to the ground. A 3636 kg capacity electric winch with cable (Chicago Tools, Chicago, IL, USA) was secured to a 1 m high wooden platform located 13 m east of the branch pulling apparatus. The rope was attached to the cable and the winch was activated, pulling the branch downward until failure was audibly

detected from the position of the winch. The winch retracted the cable at a displacement rate of approximately 8 cm/s. Load cell measurements were sampled at 20 Hz using a 16-bit data acquisition system and recorded on a laptop computer running LabView software (National Instruments Corporation, Austin, TX, USA). Forces recorded at each pull point were compared to the force recorded by the terminal load cell at pulley 9, and were used to calibrate force distribution in the branch pull test. All branches were pulled within one hour of removal from the tree.

Branch pull test

Ten primary branches (mean diameter = 4.9 cm, SD ± 0.73; mean length = 4.4 m, SD ± 0.72; attachment angle ranged from 40° to 50°) were selected from each of the same two trees described earlier. Reorientation treatment (horizontal or vertical) was randomly assigned to the branches (2 orientation treatments × 2 trees × 5 branches per treatment per tree = 20 branches). Branches (one at a time) were removed from the trees at the trunk and taken to the branch pulling station, secured in the mounting bracket (Fig. 1) on the vertical post (Fig. 2). Attachment angle (measured from the post above the branch to the branch; Fig. 3) for horizontal reoriented branches ranged from 76° to 89°; angles of those pulled from the vertical reorientation ranged from 6 to 29. Branch angles were measured by placing a digital level on the tops of branches distally adjacent to the steel mounting bracket. Primary branch diameter at the base (distally adjacent to the steel mounting bracket) and at each of the three pull points was measured with a diameter tape. The three-point pull system was attached to branches and the angle iron below as described in the load distribution test and the rope was connected to the winch cable. The winch retracted the cable at a displacement rate of approximately 8 cm/s with the electric winch pulling the branch downward until audible failure occurred. Time from starting the winch until audible failure ranged from 44 to 108 s. All branches were pulled within one hour of removal from the tree. A Canon PowerShot SX 10IS camera (Canon Inc., Tokyo, Japan) was placed 8 m east of the approximate center of the branch

at a height of 2 m from the ground and video recordings were made for each branch test. The bottom of the view finder was parallel to the ground.

Applied force at failure was calculated using the following formula:

$$F_A = F_M \times \frac{\sqrt{2}}{2} \tag{1}$$

where F_A is applied force and F_M is the force measured by the load cell at the terminal end of the angle iron. This equation was used because the rope went through pulley 9 at a right angle, so the resultant force is the vector sum of rope tension parallel and perpendicular to the angle iron.

After branch failure occurred, branches were lowered to the ground. Diameter of the failure point was measured with a diameter tape proximally adjacent to the visible crack that occurred about perpendicular to the branch axis on the branch top. Two branches failed in a manner which caused them to splinter longitudinally along the primary branch. Both branches broke into three separate pieces. In these cases, branches were manually reassembled and secured in a vise, approximately restoring them to their pre-failure diameter. Branch diameters were then measured with a diameter tape proximally adjacent to the visible failure point on the branch tops.

To measure branch angle at the point of failure, video recordings were played on a screen, frame by frame, as failure occurred. Recordings were paused on the frame immediately prior to failure. This frame of the video was referred to as the failure frame. The point of failure on the branch was temporarily marked on the video screen. A straight edge ruler was secured to the screen visually tangent to the point of failure on the top of the branch. The angle formed by a horizontal line and tangent line was considered to be the branch angle (θ) at the point of failure (Fig. 3). A digital level was used to ensure the screen was horizontal. The digital level was placed on the straight edge ruler and the angle was recorded. Branch angle change at each of the three pull points was determined by measuring initial angle at each pull point and the angle at failure for each pull point. Branch angle at failure was subtracted from initial angle to calculate change in branch angle.

Five vertical lines were fixed to the image in the failure frame, one at the branch base, one at the failure point, and one at each of the three pull points. The horizontal distance from the vertical line at the branch base to the vertical line at the failure point, and from branch base to each pulling point was measured by using the distance between holes on the angle iron mounted to the platform (5 cm) for scale. The vertical distances from the ground (i.e., the angle iron on the platform) to pull points and from the ground to the failure point were measured parallel to the vertical post using the aforementioned lines marked on the vertical post for scale. These horizontal and vertical distances were used to calculate bending moment (M) in Eq. (4) below.

The horizontal component of force (H_N) at each pull point was calculated using the following equation:

$$H_N = F_N(\sin(\alpha_N)) \tag{2}$$

where α_N is the rope angle from vertical measured on the failure frame, with the subscript (N) indicating that this calculation was made for each pull point (Fig. 3). F_N represents 22.5%, 51.7%, and 96.5% of F_A for the proximal, middle, and distal pull points, respectively (rationale explained in Results and discussion section).

The vertical component of force (V_N) at each pull point was calculated using the following equation:

$$V_N = F_N(\cos(\alpha_N)) \tag{3}$$

Applied force measured from Eq. (1) was converted to bending moment (M):

$$M = H_1(y_B - y_1) + H_2(y_B - y_2) + H_3(y_B - y_3) - V_1(x_1 - x_B)$$
$$- V_2(x_2 - x_B) - V_3(x_3 - x_B) \tag{4}$$

where H_1, H_2, and H_3 are the horizontal components of force for proximal, middle, and distal pull points at failure, respectively. V_1, V_2, and V_3 are the vertical components of force for proximal, middle, and distal pull points at failure, respectively. y_1, y_2, and y_3 are the vertical distances from the ground to proximal, middle, and distal pull points, at failure, respectively. x_1, x_2, and x_3 are the horizontal distances from the branch base at the edge of the bracket to proximal, middle, and distal pull points at failure, respectively. y_B is the vertical distance from breakpoint to the ground. x_B is the horizontal distance from the branch base to the breakpoint.

Bending stress (σ_b) was calculated using the following equation:

$$\sigma_b = \frac{M(y)}{I} \tag{5}$$

where y is the distance from the neutral axis to the failure point, and the formula for I (second moment of area) is:

$$I = \frac{\pi r^4}{4} \tag{6}$$

where r is the branch radius at point of failure. Bending stress is tensile in the portion of the branch above the longitudinal neutral axis (top) and compressive in the portion below the neutral axis (bottom). Tensile stress is taken to be positive and compressive stress is taken to be negative (Hibbeler, 2005).

To calculate axial force (P), the following equation was used:

$$P = [(H_1 + H_2 + H_3)(\cos\ \theta) - (V_1 + V_2 + V_3)(\sin\ \theta)] \tag{7}$$

where θ is the branch angle (Fig. 3) at the point of failure.

Axial force was used to determine axial stress using the following equation:

$$\sigma_a = \frac{P}{\pi r^2} \tag{8}$$

Bending stress and axial stress were used to calculate breaking stress (σ_T):

$$\sigma_T = \sigma_b + \sigma_a \tag{9}$$

Axial stress was considered positive when the angle between the branch distal to the pull point and the rope at that pull point (α_N) was less than 90°, and negative when the angle was greater than 90° (Fig. 3). The experimental configuration prevented reliable estimation of the change in the neutral axis (i.e., $d\theta/dx$ could not be determined from visual observations), therefore Table 1 shows the resultant stress in the extreme fiber of the branch for the case where the neutral axis aligns with the centroid of the cross section. For branches that failed between the proximal and middle pull-points, the proximal component of the stress equations was excluded from analysis because the force at the proximal pull point did not affect failure of those branches.

Branch taper for the middle and distal pull points was calculated using the equation:

$$\text{Taper} = -\frac{(R - r)}{RL} \tag{10}$$

where R is branch radius at the edge of the mounting bracket, r is the branch radius at the pull point, and L is the length between the edge of the mounting bracket and the pull point (Leiser and Kemper, 1973).

Analysis of variance (ANOVA) tested differences in breaking stress between branch reorientations, distance along primary branch from edge of the bracket to the failure point, basal

Table 1
Branch attributes and breaking stress by reorientation.

Branch reorientation[a]	Basal branch diameter (cm)	Branch length (m)	Branch diameter at failure point (cm)	Distance to failure point (cm)[b]	Breaking stress (MPa)
Horizontal	4.9 (0.74)a	4.52 (0.75)a	4.7 (0.73)a*	10.5 (19.3)a***	64 (25.2)a**
Vertical	5.0 (0.77)a	4.35 (0.71)a	4.0 (0.55)b	74.4 (46.7)b	32 (8.7)b

Note: Means in a column with different letters are significantly different at *$p < 0.05$; **$p = 0.001$; ***$p < 0.0005$. Standard deviation (SD) in parentheses.

[a] Horizontal branch departure angles ranged from 76° to 89°; vertical branch departure angles ranged from 6° to 29°.

[b] Distance to break = distance from edge of mounting bracket to point of failure.

branch diameter, and total branch length. The model tested was response = reorientation + branches (reorientation); tree effect was pooled because it did not impact any measured parameter. A separate ANOVA for each pull point tested for differences between reorientations in branch angle change from start of branch pull test to branch failure. ANOVA was performed to test differences in taper between reorientations, between pull points, and the interaction between reorientation and pull point. Fisher's exact test evaluated the influence of branch reorientation on location of failure which had two values (1) between branch base and proximal pull point, or (2) between proximal and middle pull point. Statistical analyses were performed in SAS version 9.2 (SAS Institute, Cary, NC) using the PROC GLM and FREQ procedures. Mean separations were analyzed using Tukey's highly significant difference test. Differences were considered significant at a level of $\alpha = 0.05$.

Results and discussion

Branches at all eight positions along the main axis traveled the same distance whether static loaded or pulled with the three-point pull system (data not shown, $p = 1$ for both horizontal and vertical branches). This indicates that the three-point pull system was a valid method for simulating a distributed static load on *L. tulipifera* branches within the elastic range of this test. Previous single-point pull studies often pulled from a position close to the union (MacDaniels, 1923; Smiley, 2003; Gilman, 2003) or further out (Dahle et al., 2006; Kane, 2007) on the branch, forcing branches to break closer to the union than they may have failed under a natural distributed static load such as ice or snow. Although not reported on previously, it is possible that naturally accreting loads may be distributed differently along a branch than in the manner applied in the present study. However, the results of the three-point pull system may be more consistent with at least some observed natural branch failure than single-point pull systems. Beyond the elastic range, it was not possible to validate the three-point pull system with branch deflection from static loading on the same branch due to fiber failure.

During the load distribution tests, force recorded at the distal pull point on the branch (pulley 7) was 96.5% (SD = 6.4) of the force calculated from the terminal load cell (pulley 9) at the end of the platform when failure occurred. Forces at the middle and proximal pull points were 51.7% (SD = 4.1) and 22.5% (SD = 4.7) of the force calculated from the terminal load cell, respectively (data not shown). The reduction in force from the distal to proximal pull points was likely the result of friction in the pulley system, the large deflection of branches, and the mechanical advantage of the pulley system. Based on the results of this force distribution calibration, force values used in stress calculations (Eq. (9)) for the distal, middle, and proximal pull points were 96.5%, 51.7% and 22.5%, respectively, of applied force from Eq. (1).

Orientation significantly impacted break location ($p < 0.01$). Seven of the ten vertical branches broke between the proximal and middle pull points, whereas only one of the ten horizontal branches broke at that position. These eight failures occurred distally adjacent to (within 5 cm) the proximal pull point where lateral branches with diameters at least one-third that of the broken primary branch

originated. The other three vertical branches and nine horizontal branches broke between the edge of the mounting bracket and the proximal pull point. Branches may have broken in a different manner had the lateral branch at the proximal pull point also been loaded.

Breaking stress for horizontal reoriented branches (64 MPa) was larger than for vertical reoriented branches (32 MPa) ($p = 0.001$; Table 1). The experimental configuration prevented reliable estimation of the change in the neutral axis (i.e., $d\theta/dx$ could not be determined from visual observations), therefore Table 1 shows the resultant stress in the extreme fiber of the branch for the case where the neutral axis aligned with the centroid of the cross section. Previous studies used a similar methodology to calculate stress on branches (Lilly and Sydnor, 1995; Dahle et al., 2006), although displacements were not reported in those studies. Recent research on bending stress of tree stems also assumes a circular cross-section (Smiley et al., 2012). When loading Bradford pear branches to failure, Kane (2007) reported that the distance from the trunk to the loading point on the pulled branch was a minimum of 1 m, and the load was applied at a rate of 0.4 m/s for 5–10 s (which would equal approximately 2–4 m of deflection assuming the rope was low-stretch and not slack when pulling began). However, no amount of total deflection was reported. Future research could investigate an experimental configuration that allows for a more precise estimation than the current and previous studies. It is also important to note that because large deflections occurred during testing, we applied an equilibrium equation using the deformed shape of the branch to calculate the internal forces. Although other structural analysis techniques exist (e.g., Morgan and Cannell, 1988), our experimental methodology prevented us from utilizing other methods of analysis, which may be a limitation to this study.

Average distance from the edge of the mounting bracket to the failure point measured along the primary branch was six times greater for vertical branches than horizontal branches ($p < 0.0005$; Table 1). Therefore, the diameter of the branch at the break point was smaller for vertical (4.0 cm) than horizontal (4.7 cm) branches ($p < 0.05$; Table 1) because branch diameter tapers in the distal direction, with marked decreases in diameter occurring at lateral branch unions. This sudden reduction in diameter likely focused loading just beyond the first lateral branch union on vertically reoriented branches. Small differences in diameter result in relatively large differences in stress, because branch radius is raised to the 4th power when calculating stress (Eq. (6)). Although not measured, it is possible that the juvenile:mature wood ratio was greater at the point of failure for vertically reoriented branches because failures tended to occur further from the branch base, and juvenile wood is typically weaker than mature wood (Adamopoulos et al., 2007). Future research should examine the effect of juvenile:mature wood ratio on branch breaking strength.

Taper from the bracket to any of the pull points was not different between reorientations ($p = 0.7464$). Among all branches, however, taper was less from the edge of the mounting bracket to the proximal pull point than from the bracket to the middle and distal pull points ($p < 0.005$). This was expected because there were no lateral branches between the bracket and the proximal pull

Table 2
Branch angle change to failure during pull test.

Branch reorientation	Angle change (in degrees) for each pull point		
	Proximal	Middle	Distal
Horizontal	42.5 (15.7)a*	60.2 (9.2)a**	60.3 (9.6)a***
Vertical	23.8 (19.8)b	76.2 (11.8)b	88.2 (12.5)b

Note: Means in a column with different letters are significantly different at $^*p < 0.05$; $^{**}p < 0.005$; $^{***}p = 0.0001$. Standard deviations (SD) in parentheses.

point; whereas there were several branches between the bracket and the middle and distal pull points. There was no difference in taper from the edge of the bracket to the middle and distal pull points. Leiser and Kemper (1973) point out that location of maximum bending stress on sapling trunks can be affected by taper, although Kane (2007) found no effect of taper on breaking stress in Bradford pear branches. Seven vertically reoriented branches and one horizontally reoriented branch failed beyond the proximal pull point along the portion of the branch that had greater taper. The other twelve branches failed between the mounting bracket and the proximal pull point where taper was less. Given the difference in break location between reorientation treatments without a difference in taper, it is unclear what effect taper had on breaking stress or break location in the present study. Further research into effects of taper on branch failure is warranted.

Angle change from the time the pull started until the time of failure for vertical branches was larger than for horizontal branches at the middle ($p < 0.005$) and distal ($p = 0.0001$) pull points. However, angle change at the proximal pull point was smaller for vertical than horizontal oriented branches ($p < 0.05$; Table 2). This indicates that horizontal branches bent more uniformly from the distal pull point to the mounting bracket, allowing stress to be distributed along the branch back toward its base where diameter was greater. In contrast, vertical branches experienced large changes in angle at the distal and middle pull points with little change at the proximal pull point. The lack of angle change in the proximal portion of vertical branches coupled with the large angle change at the distal and middle pull points resulted in an acute bend that focused bending stress (on 9 out of 10 branches) just beyond the proximal pull point (Fig. 3) causing branches to fail in that region. This failure pattern appears to be similar to damage that often occurs during storms.

There is conflict in the literature as to what extent branch wood properties may be affected by branch attachment angle. Kane (2007) reanalyzed MacDaniels (1923) data and found that breaking stress was larger for more horizontally oriented branches than those with a more vertical orientation, which appears to support findings in the present study. However, Kane (2007) found no relationship between attachment angle and breaking stress for *P. calleryana* 'Bradford' branches ranging in diameter from 7.1 to 17.8 cm. The range in attachment angle in that study was 13–61°, whereas reoriented branch angles in the present study were mostly outside of this range at 76–89° for horizontal branches and 6–29° for vertical branches. The difference in diameter or range of attachment angles between the present study and that study may partly explain the discrepancy. Moreover, reaction wood amount or position may have varied in Kane (2007) among the branch samples naturally displayed at different angles, but was probably more consistent among branches in the present study due to the narrow range (40–50°) in natural attachment angle of sample branches prior to removing them from source trees.

Dahle and Grabosky (2010) found no difference in *E* between wood samples extracted from the tops of branches containing tension wood and wood samples from the bottom that lacked tension wood. Sone et al. (2006) found that *E* was negatively correlated with attachment angle (upright branches were stiffer than more

horizontal branches), but did not test for reaction wood. Selecting branches within a narrow angle range allowed us to isolate the impact of reorientation on breaking strength by minimizing the variability in the amount of tension wood among branches. Although branches in the present study were not tested for tension wood, previous work showed that tension wood developed on the upper sides of the stems when young vertical stems of *L. tulipifera* were reoriented to 45° (Jin and Kwon, 2009), similar to the branch angle of sample branches on the two source trees in the current study. Future studies should investigate the influence of attachment angle on formation of reaction wood in branches, and presence of reaction wood on breaking strength.

Breaking stress in the present study may have been underestimated because branches were assumed to be circular in cross section. Kane (2007) found bending stresses to be larger when branch cross sections were considered elliptical (i.e., measured width and depth) rather than circular. Although calculated stress values in the current study may be less than if branches were considered elliptical, comparisons between orientations remain valid because the range of natural attachment angles on source trees was small (40–50°). Thus, any underestimation of breaking stresses resulting from considering branch cross sections as circular would have been equally applied to all branches, and reorientation treatments (vertical or horizontal) of removed branches were randomly assigned.

One consideration in evaluating these results is that branch fibers distal to the failure point may have stretched beyond their elastic limit without failing audibly. Audible cracking was the indicator of failure in the present study. However, the wood in the distal portion of the branch may have failed inaudibly prior to audible failure due to their small diameter, as Dahle and Grabosky (2010) report a lower *E* at the distal 2–3 m for slightly larger diameter branches of *A. platanoides*. The distal pull point in the present study was located within the section of potentially lower *E* (distal 2.5 m). This may have contributed to the acute bending that occurred in the vertically reoriented branches. Inaudible failure was unlikely, however, because force never decreased at any time during the pull and there were no signs of bark cracking other than at the failure point. External cracks perpendicular to the branch axis occurred on the tops of branches at the failure point and bark buckling perpendicular to the branch axis occurred on the underside of many branches. It is also important to note that torsion was not investigated in the present study. Although very little torsion was visually detected, it is possible that torsional stresses occurred during testing. Effect of torsional stress on branch strength is recommended in future studies.

Findings from this study may help to explain why vertical branches are damaged more often than horizontal branches in ice and snow storms. When structurally pruning trees, arborists may consider reducing upright branches back to lateral branches in an effort to develop a more horizontal branching pattern. Potential improvement in tree structure from pruning should be balanced against the likelihood of decay developing behind reduction cuts, especially in species that are weak compartmentalizers (Grabosky and Gilman, 2007). It is important to note that branches in this study were not pulled from their natural orientation, and adaptive growth by branches at different natural orientations may influence load bearing capacity. Future studies should investigate branches in their natural orientation to determine the contribution of orientation and reaction wood to breaking stress. It is also important to note that results from this study should not be extrapolated beyond *L. tulipifera* branches within a small diameter range (mean diameter = 4.9 cm, SD ± 0.73) growing in northern Florida. Further research on breaking strength of larger branches and on other species would benefit the body of knowledge in this area of tree biomechanics.

Acknowledgments

References

Adamopoulos, S., Passialis, C., Voulgaridis, E., 2007. Strength properties of juvenile and mature wood in black locust (*Robinia pseudoacacia* L.). Wood Fiber Sci. 39, 241–249.

Bruederle, L.P., Stearns, F.W., 1985. Ice storm damage to a southern Wisconsin mesic forest. Bull. Torrey Bot. Club 112, 167–175.

Coutand, C., Jeronimidis, G., Chanson, B., Loup, C., 2004. Comparison of the mechanical properties of tension and opposite wood in *Populus*. Wood Sci. Technol. 38, 11–24.

Dahle, G.A., Holt, H.H., Chaney, W.R., Whalen, T.M., Cassens, D.L., Gazo, R., McKenzie, R.L., 2006. Branch strength loss implications for silver maple (*Acer saccharinum*) converted from round-over to V-trims. Arboricult. Urban For. 32, 148–154.

Dahle, G.A., Grabosky, J.C., 2010. Variation in modulus of elasticity (*E*) along *Acer platanoides* L. (Aceraceae) branches. Urban For. Urban Green. 9, 227–233.

Du, S., Yamamoto, F., 2007. An overview of the biology of reaction wood formation. J. Integr. Plant Biol. 49, 131–143.

Duryea, M.L., Kampf, E., Littell, R.C., 2007. Hurricanes and the urban forest. I. Effects on southeastern United States coastal plain tree species. Arboricult. Urban For. 33, 83–97.

Fisher, J.B., Stevenson, J.W., 1981. Occurrence of reaction wood in branches of dicotyledons and its role in tree architecture. Bot. Gaz. 142, 82–95.

Gilman, E.F., 2003. Branch-to-stem diameter ratio affects strength of attachment. J. Arboricult. 29, 291–294.

Grabosky, J.C., Gilman, E.F., 2007. Response of two oak species to reduction pruning cuts. Arboricult. Urban For. 33, 360–366.

Green, D.W., 2001. Wood: strength and stiffness. In: Encyclopedia of Materials: Science and Technology., ISBN 0-08-0431526, pp. 9732–9736.

Gurau, L., Cionca, M., Mansfield-Williams, H., Sawyer, G., Zeleniuc, O., 2008. Comparison of the mechanical properties of branch and stem wood for three species. Wood Fiber Sci. 40, 647–656.

Hauer, R.J., Wang, W., Dawson, J.O., 1993. Ice storm damage to urban trees. J. Arboricult. 19, 187–194.

Haygreen, J.G., Bowyer, J.L., 1996. Forest Products and Wood Science, 3rd ed. Iowa State University Press, Ames, IA, pp. 484.

Hibbeler, R.C., 2005. Mechanics of Materials, 6th ed. Prentice Hall Inc., Upper Saddle River, NJ, pp. 873.

Jin, H., Kwon, M., 2009. Mechanical bending-induced tension wood formation with reduced lignin biosynthesis in *Liriodendron tulipifera*. J. Wood Sci. 55, 401–408.

Kane, B., 2007. Branch strength of Bradford pear (*Pyrus calleryana* var. 'Bradford'). Arboricult. Urban For. 33, 283–291.

Kane, B., Farrell, R., Zedaker, S.M., Loferski, J.R., Smith, D.W., 2008. Failure mode and prediction of the strength of branch attachments. Arboricult. Urban For. 34, 308–316.

Leiser, A.T., Kemper, J.D., 1973. Analysis of stress distribution in the sapling tree trunk. J. Am. Soc. Hortic. Sci. 98, 164–170.

Lilly, S., Sydnor, T.D., 1995. Comparison of branch failure during static loading of silver and Norway maples. J. Arboricult. 21, 302–305.

MacDaniels, L.H., 1923. The Apple-tree Crotch. Bulletin 419. Cornell University Agricultural Experiment Station, Ithaca, NY.

Menuccini, M., Grace, J., Fioravanti, M., 1997. Biomechanical and hydraulic determinants of tree structure in Scots pine: anatomical characteristics. Tree Physiol. 17, 105–113.

Morgan, J., Cannell, M.G.R., 1988. Support costs of different branch designs: effects of position, number, angle and deflection of laterals. Tree Physiol. 4, 303–313.

Niklas, K.J., 1992. Plant Biomechanics. University of Chicago Press, Chicago, IL.

Niklas, K.J., 1997. Mechanical properties of black locust (*Robinia pseudoacacia* L.) wood: correlations among elastic and rupture moduli, proportional limit, and tissue density and specific gravity. Ann. Bot. 79, 479–485.

Putz, F.E., Coley, P.D., Lu, K., Montalvo, A., Aiello, A., 1983. Uprooting and snapping of trees: structural determinants and ecological consequences. Can. J. Forest Res. 13, 1011–1020.

Rebertus, A.J., Shifley, S.R., Richards, R.H., Roovers, L.M., 1997. Ice storm damage to an old-growth oak-hickory forest in Missouri. Am. Midland Nat. 137, 48–61.

Ruel, J.-C., Achim, A., Herrera, R.E., Cloutier, A., 2010. Relating mechanical strength at the stem level to values obtained from defect-free wood samples. Trees 24, 1127–1135.

Ruelle, J., Beauchene, J., Thibaut, A., Thibaut, B., 2007. Comparison of the physical and mechanical properties of tension and opposite wood from ten tropical rainforest trees from different species. Ann. Forest Sci. 64, 503–510.

Ruelle, J., Beauchene, J., Yamamoto, H., Thibaut, B., 2011. Variations in physical and mechanical properties between tension and opposite wood from three tropical rainforest species. Wood Sci. Technol. 45, 339–357.

Schmidlin, T.W., 2009. Human fatalities from wind-related tree failures in the United States, 1995–2007. Nat. Hazards 50, 13–25.

Sellier, D., Fourcaud, T., 2009. Crown structure and wood properties: influence on tree sway and response to high winds. Am. J. Bot. 96, 885–896.

Shigo, A.L., 1985. How tree branches are attached to trunks. Can. J. Bot. 63, 1391–1401.

Smiley, E.T., 2003. Does included bark reduce the strength of codominant stems? J. Arboricult. 29, 104–106.

Smiley, E.T., Kane, B., Autio, W.R., Holmes, L., 2012. Sapwood cuts and their impact on tree stability. Arboricult. Urban For. 38, 287–292.

Sone, K., Noguchi, K., Terashima, I., 2006. Mechanical and ecophysiological significance of the form of a young *Acer rufinerve* tree: vertical gradient in branch mechanical properties. Tree Physiol. 26, 1549–1558.

USDA Forest Service, 2010. Wood Handbook – Wood as an Engineering Material. FPL-GTR-113. U.S. Department of Agriculture, Forest Service, Forest Products Laboratory, Madison, WI, pp. 463.

Wilson, B.F., Archer, R.R., 1977. Reaction wood: induction and mechanical action. Annu. Rev. Plant Physiol. 28, 23–43.